Available online at www.HighTechJournal.org

HighTech and Innovation Journal

ISSN: 2723-9535

Vol. 7, No. 1, March, 2026

Tourism Ecological Environment Quality Assessment Using Principal Component Analysis and Remote Sensing Data

Ruiping Chen [1*], Xiang Wei [2], Wei Wang [1]

[1] *School of Culture Tourism and Creativity, Foshan Polytechnic, Foshan, 528137, China.*

[2] *National Academy of Economic Strategy, Chinese Academy of Social Sciences, Beijing 100028, China.*

Received 17 September 2025; Revised 19 January 2026; Accepted 29 January 2026; Published 01 March 2026

Abstract

Current methods for assessing tourism ecological environment quality suffer from insufficient analysis of complex environmental impact factors and low assessment accuracy. In response to this situation, this study proposes a method for assessing tourism ecological environment quality that takes into account principal component analysis and remote sensing data. The study first combined remote sensing data and principal component analysis to establish an evaluation index system, and then introduced the grey-scale correlation method to rank and assign weights to key factors affecting ecological environment quality. Based on the results of principal component analysis and the grey-scale correlation method, the study constructed a comprehensive assessment model. Subsequently, dynamic simulation and prediction were achieved by combining the meta-cellular automata model and the Markov model. The experimental results indicated that in the ecological assessment of different seasonal environments, the Kappa coefficient and overall accuracy of the proposed method reached 0.93 and 0.93, respectively. Furthermore, the coefficient of determination and mean absolute percentage error were 0.91 and 0.08, respectively, and the assessment accuracy reached 93.88%. The tourism ecological environment quality assessment method proposed in this study can effectively address challenges in different environments. It maintains high-precision assessments and dynamic predictions, providing a reliable basis for decision-making in ecological environment protection.

Keywords: Remote Sensing; Tourism; Ecological Environment; Principal Component Analysis; Quality Assessment; Markov Model.

1. Introduction

With the continuous development of the social economy, tourism has gradually become an important means of leisure and entertainment for people. Moreover, the quality of the tourism ecological environment (Eco-E) has also become an important indicator for measuring the attractiveness of a tourism destination [1]. Ecological balance has been disrupted, vegetation coverage has decreased, and water pollution and other issues have become increasingly prominent [2]. As science, technology, and artificial intelligence have advanced, assessing ecological environment quality (EEQ) has steadily gained popularity among academics [3, 4]. Existing tourism ecological quality assessment methods mostly rely on traditional statistical data, lacking real-time and dynamic characteristics. Additionally, existing methods cannot fully consider the interactions between various factors when dealing with complex environmental factors, leading to biases in assessment results [5, 6]. Sun et al. conducted a quality assessment of the regional environment by integrating multiple remote sensing indicators in order to achieve ecological quality evaluation. This method combined classification algorithms to judge remote sensing images and draw time series diagrams. This enabled the evaluation of EEQ. The

* Corresponding author: chrp_chen@outlook.com

https://doi.org/10.28991/HIJ-2026-07-01-06

results showed that this method could provide effective information for policymakers and authorities to implement it [7]. Li et al. proposed a method for evaluating and predicting urban green space planning schemes based on the particle swarm optimization algorithm and the backpropagation neural network. This method used the PSO algorithm to optimize the neural network model parameters and used the model to learn and evaluate landscape planning. The results showed that the evaluation accuracy of this method reached 94.11% [8].

Remote sensing technology is widely used to obtain large-scale surface information in various fields [9]. In order to conduct precise measurements of trees and forests, Lines et al. proposed a method of constructing three-dimensional models using remote sensing data to capture the details of tree canopies and reveal the complex interactions among trees. This method precisely reproduced the shape of the tree crown through high-resolution images and lidar data. The results showed that the accuracy of the data obtained by this method reached over 90% [10]. Pan et al. used remote sensing technology to monitor the proliferation of green algae in the Yellow Sea area in an attempt to explore the growth patterns and distribution of green algae. This method combined deep learning methods to analyze remote sensing images, estimate the biomass of green algae, and measure its drift velocity. The results showed that this method could promote the development of remote sensing technology and assist in disaster prevention and ecological protection [11]. Lu et al. proposed an ecological evaluation model for urban green Spaces that integrated multi-source remote sensing data in order to accurately assess the ecological benefits of urban green Spaces. This model adopted remote sensing data and ground measured data, combined with machine learning methods, to comprehensively assess the green space coverage rate, vegetation health status, and ecological service functions. The results showed that the accuracy rate of the model in multiple city applications exceeded 85% [12].

Yu et al. proposed a satellite monitoring method based on quantitative remote sensing sensing transformers to improve the accuracy of forest carbon storage monitoring. This method combined the attention mechanism and style transformation technology to process images. The results showed that the monitoring accuracy after the application of this method was improved by 10.33% compared with traditional prevention [13]. In order to understand the effects of climate, topography, soil, and human factors on remote sensing ecological indices, Pan, J., et al. monitored and analyzed climate change and mining activities in mining areas. They based their analysis on data extracted by the partial least squares model and Google Earth Engine. The results showed that human variables did not have a negative impact on the ecological index of sludge [14]. Shu et al. proposed a new convolutional neural network architecture for Yu Xiao to assess the groundwater quality and environmental conditions in Lahore, Pakistan. This architecture adopted a multi-scale feature fusion strategy to extract the spatial distribution characteristics of groundwater pollution. The results showed that this model, combined with remote sensing images, could accurately identify the degree of groundwater pollution [15]. In response to the current problems of data integration, scale differences, and low accuracy and timeliness in ecological and climate monitoring, Han et al. conducted a comprehensive analysis of the latest progress in multi-source remote sensing data fusion technology and spatio-temporal matching algorithms. The analysis results showed that the fusion of multi-source data significantly improves the spatiotemporal resolution and accuracy of environmental monitoring [16]. Zhou et al. found that in remote lands and at sea, remote sensing monitoring still had difficulty achieving continuous observation with high frequency and high precision. It proposed two innovative ways to cover Internet of Things (IoT) services, enhancing service coverage through iot data collection and remote sensing based on IoT. The results showed that the remote sensing monitoring method combined with the Internet of Things could effectively increase the frequency of data acquisition and the continuity of spatial coverage [17].

Based on the literature mentioned above, it is clear that incorporating remote sensing technology into current methods of assessing the quality of the Eco-E has significant advantages, especially for large-scale, dynamic, and multidimensional monitoring, for which it plays an irreplaceable role. However, existing EEQ assessment methods based on artificial intelligence and remote sensing images still face challenges, including insufficient model generalization ability, an imperfect multi-source data fusion mechanism, and poor real-time performance. Some studies rely on specific regional samples for training. This leads to a decline in accuracy when the studies are applied across regions. The studies also have weak adaptability to complex terrains and extreme climates. In addition, the existing models have relatively low computational efficiency when dealing with high spatiotemporal resolution data, making it difficult to meet the requirements of dynamic monitoring. To address this issue, the research uses principal component analysis (PCA) and remote sensing data to assess the quality of the tourism Eco-E and explore the key factors influencing it. The innovation of this study lies in its in-depth understanding of the patterns of Eco-E changes within the region and the proposal of a new evaluation index system. Additionally, the study uses a combination of cellular automata and Markov models to simulate and predict dynamic changes in the quality of the Eco-E. This provides a scientific basis for the sustainable development (SD) of tourist destinations. The study aims to provide reliable decision-making basis for ecological management in tourist areas by analyzing EEQ.

The study is divided into three sections. The first section is the methodology section, which provides a detailed introduction and description of the proposed EEQ assessment method. The second section is the experimental analysis section, where the proposed method is subjected to simulations and comparative experiments in real-world scenarios. The third section is the conclusion, which summarizes the research findings and experimental results. It also analyzes the limitations of the method and suggests future research directions.

2. Material and Methods

The study constructs an EEQ evaluation system for tourism based on PCA and RSD. On this basis, meta-cellular automata, Markov models, and geographically weighted regression (GWR) models are combined to dynamically predict and evaluate EEQ.

2.1. RSD Collection and EEQ Evaluation System

In ecological and environmental quality assessment, RSD collection is of critical importance. RSD contains rich spectral information and spatial resolution, enabling precise reflection of surface vegetation coverage, water body distribution, and soil conditions. A comprehensive analysis of this information effectively reveals the current state of regional ecological and environmental conditions, providing a solid foundation for constructing a scientifically reasonable evaluation indicator system. The study utilizes RS imagery data from the United States Geological Survey (USGS) as its data foundation. The study selects a typical tourist island in China as the research object, utilizing Landsat 8 satellite data for image acquisition. Preprocessing is conducted using ENVI software, including radiometric correction, geometric correction (GC), and atmospheric correction (AC), to ensure data accuracy. The data acquisition timeframe spans from 2021 to 2024. The changes in ecological and environmental indicators for this region are shown in Figure 1 [18].

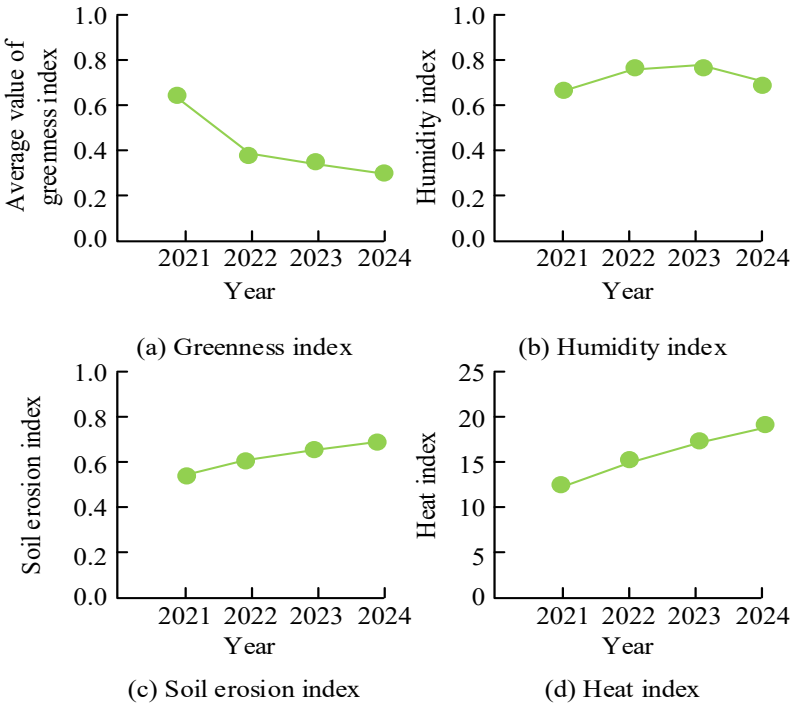

Figure 1. The changes in the Eco-E indicators of the region

In Figure 1(a), the average greenness index value for the study area in 2021 is 0.62, 0.39 in 2022, 0.35 in 2023, and drops to 0.28 in 2024. In Figure 1(b) and (c), the humidity index and soil erosion index shows fluctuating downward and upward trends, respectively. In Figure 1(d), the heat index for this region also shows an upward trend year by year. After collecting RSD, the study uses radiation calibration, AC, and image cropping for preprocessing. Radiometric calibration (RC) converts the grey values in RS images into reflectance using RC coefficients to ensure data consistency. The study uses the fast line-of-sight atmospheric analysis of spectral hypercubes (FLLAASH) model to perform AC on the radiometrically calibrated images. Finally, the study uses vector boundary files of the region to crop the original images and extract the specific scope of the study area. The study initially selects key indicators such as regional greenness, humidity, soil erosion index, heat, dryness, and vegetation coverage to construct a comprehensive evaluation index. These indicators are important parameters reflecting the regional Eco-E status and can accurately quantify Eco-E changes with the support of RSD. However, the weights of these indicators need to be determined through PCA. PCA can effectively extract the main components of the data, reduce the redundancy of indicators, and retain the vast majority of the variance of the original information at the same time. It is suitable for ecological data with strong correlations among multiple indicators. Through grey relational degree analysis, GRA can reveal the dynamic correlation characteristics

between each index and changes in the Eco-E, making up for the deficiency of PCA in identifying nonlinear relationships. The combination of the two can achieve the scientificity and objectivity of weight distribution, and enhance the accuracy and reliability of the evaluation model. Therefore, the study adopts a combination of PCA and GRA to assign weights to the selected indicators. The study combines the results of PCA to weight the RS ecological indicators of each component. Table 1 displays the PCA results [19].

Table 1. Principal component analysis results

Indicator	Year				Contribution rate (%)
	2021	2022	2023	2024	
Greenness	0.798	0.712	0.733	0.794	80.45
Humidity	0.542	0.543	0.552	0.524	11.02
Soil erosion index	-0.222	-0.210	-0.241	-0.253	0.26
Heat	-0.623	-0.448	-0.428	-0.262	0.80
Dryness	-0.425	-0.512	-0.284	-0.245	9.23
Vegetation coverage	0.428	0.441	0.461	0.645	0.24

In Table 1, soil greenness, moisture content, and vegetation coverage all show a positive correlation with tourism EEQ, while soil erosion index, heat index, and dryness index have a negative impact. Among these, regional greenness has the highest contribution rate, exceeding 80%. Therefore, the study weights each indicator based on its contribution rate to construct a comprehensive assessment model. Equation 1 illustrates the greenness calculation method.

$$L = \frac{\rho_1 - \rho_2}{\rho_1 + \rho_2} \tag{1}$$

In Equation 1, L is the greenness index value, ρ_1 and ρ_2 are the near-infrared and red light band reflectance. The calculation method for the moisture index is shown in Equation 2.

$$W = 0.1511\rho_3 + 0.19723\rho_4 + 0.3283\rho_2 + 0.3407\rho_1 - 0.7117\rho_5 - 0.4559\rho_6 \tag{2}$$

In Equation 2, W is the humidity index value. ρ_3 and ρ_4 is the reflectance of the blue and green light band. ρ_5 and ρ_6 is the reflectance of the shortwave infrared band I and II. The calculation method for dryness is shown in Equation 3.

$$G = (A + B)/2 \tag{3}$$

In Equation 3, G is the dryness index value. A is the building index. B is the soil index. Equation 4 illustrates how the heat index is calculated.

$$R = l \cdot \delta + b \tag{4}$$

In Equation 4, R is the thermal infrared radiation brightness value. l is the brightness value of the infrared radiation image. δ and b are the gain value and bias value, respectively. Ecological indicators, such as the green coverage rate and humidity, are obtained through adaptive adjustments based on widely adopted remote sensing index models from existing research. These models are combined with regional climate characteristics and surface coverage types. The green coverage rate is obtained through the inversion of the normalized vegetation index (NDVI), which can effectively reflect the vegetation coverage density and growth status. The humidity index integrates the sensitive response characteristics of multispectral bands to water vapor to enhance the monitoring accuracy. All indicators are based on remote sensing physical mechanisms to ensure the scientific accuracy and consistency of ecological assessment results. In addition to RS ecological indicators, key factors affecting EEQ remain important in EEQ assessment. Therefore, this study introduces grey relational analysis (GRA) to identify the main influencing factors and their intensity of influence, and uses them as auxiliary evaluation indicators. GRA is a correlation analysis method based on system behavior sequences. It reveals the intrinsic relationships between factors by calculating the correlation between each factor and the reference sequence. The study categorizes influencing factors into three major categories: meteorological, topographical, and human activities. Meteorological factors include annual precipitation, annual average temperature, annual sunshine duration, annual evaporation, and annual average relative humidity. Topographical factors include elevation and slope. Human activity factors include socioeconomic level, land use rate, population density, and agricultural development intensity. Figure 2 depicts the GRA model's structure [20].

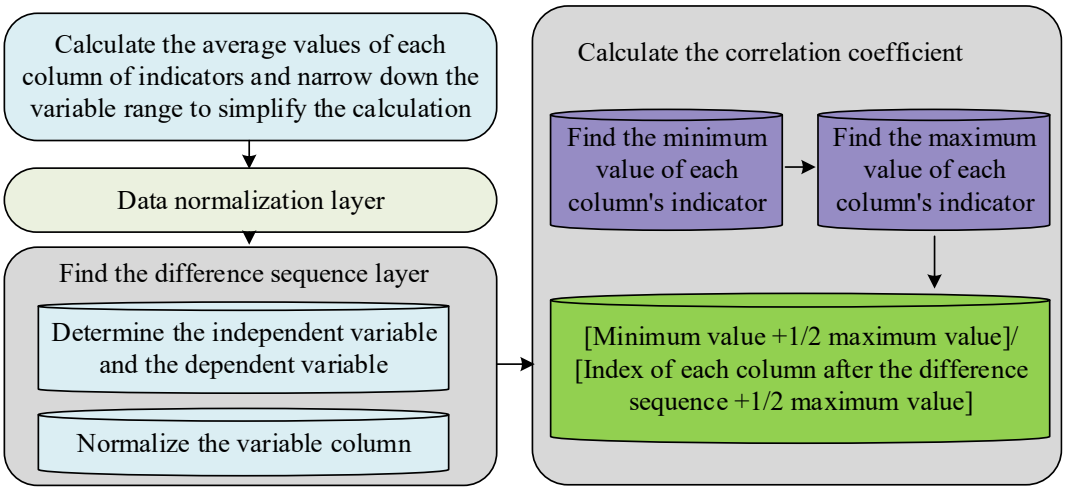

Figure 2. Grey relational analysis model structure

In Figure 2, the GRA model first calculates the average value of each column indicator, constructing a comprehensive EEQ index sequence and a sequence of influence factor indicators. Subsequently, the initialization method is used to perform dimensionless processing on the data in each sequence to eliminate differences in dimensions. The minimum and maximum discrepancies are then determined by calculating the absolute difference between the reference sequence and the comparison sequence at each time point. The calculation method for the correlation coefficient (R^2) is shown in Equation 5.

$$\xi(k_i) = (x_{\min} + \rho \cdot x_{\max}) / (\Delta x_{k_i} + \rho \cdot \rho \cdot x_{\max}) \tag{5}$$

In Equation 5, Δx_{k_i} represents the absolute difference between the i -th comparison sequence and the reference sequence at the k -th time point. x_{min} and x_{max} denote the minimum and maximum values of the absolute differences across all time points and all sequences, respectively. ρ is the resolution coefficient, with a study value of 0.5. Finally, the average R^2 for each influencing factor sequence at all time points is calculated to obtain the grey correlation degree between the factor and the comprehensive EEQ index. Using the above method, the study calculates the degree of correlation between the three major categories (meteorology, topography, and human activities), which comprise 11 specific factors, and the comprehensive EEQ index. The study then ranks them according to their degree of correlation. Table 2 displays the findings of the analysis [21].

Table 2. Grey relational analysis results of influencing factors

Categories of influencing factors	Specific factors	Grey correlation degree	Sorting
Meteorological factors	Annual precipitation	0.823	1
	Annual average temperature	0.781	3
	Annual sunshine duration	0.742	5
	Annual average relative humidity	0.698	8
	Annual evaporation	0.685	9
Topographic factors	Slope	0.712	7
	Elevation	0.662	11
Human activity factors	Intensity of agricultural development	0.798	2
	Land utilization rate	0.765	4
	Population density	0.728	6
	Socio-economic level	0.673	10

Table 2 shows that the extent of influence of various factors on ecological and environmental quality varies significantly. Among meteorological factors, annual precipitation has the highest correlation, while among topographical factors, elevation has the lowest correlation. Among human activity factors, agricultural development intensity has a significant impact, while socioeconomic level has a relatively minor impact. The study uses the ranking results to assign

weights to different influencing factors. Then, it combines these weights with the aforementioned evaluation indicator system to optimize subsequent ecological and environmental quality assessments. According to the ranking results, the weight values for each influencing factor range from 0.15 to 0.05, with annual precipitation having the highest weight and altitude having the lowest weight. The above results reveals that, the study extracts RS ecological indicators within the region and combines them with PCA to construct a comprehensive assessment index system for EEQ. Then, GRA is used to quantify the influencing factors, and the quantified results are used as their weighting standards. Finally, the influencing factors and RS indicators are combined to form a multidimensional evaluation system. The final evaluation system is shown in Table 3 [22].

Table 3. EEQ evaluation system

Indicator	Indicator weight
Greenness	0.38
Humidity	0.20
Soil erosion index	0.06
Heat	0.04
Dryness	0.05
Vegetation coverage	0.04
Meteorological factors	0.11
Topographic factors	0.04
Human activity factors	0.08

In Table 3, the study combines four RS ecological indicators and three types of key influencing factors to construct an EEQ evaluation system. It then uses GRA and PCA methods to assign weights to them.

2.2. Dynamic Prediction and Assessment of Ecological Quality Based on an Integrated Evaluation System

After extracting RSD and establishing an evaluation index system based on PCA, static evaluation can be performed on the data. However, relying solely on static evaluation is insufficient to comprehensively reflect ecological changes, necessitating the integration of time series analysis for dynamic prediction. Therefore, this study employs meta-cellular automata and Markov models to conduct dynamic prediction and assessment of EEQ. The meta-cellular automata model is a spatial dynamic model based on neighborhood interactions, capable of simulating the spatio-temporal evolution of complex systems [23]. Its composition is shown in Figure 3 [24].

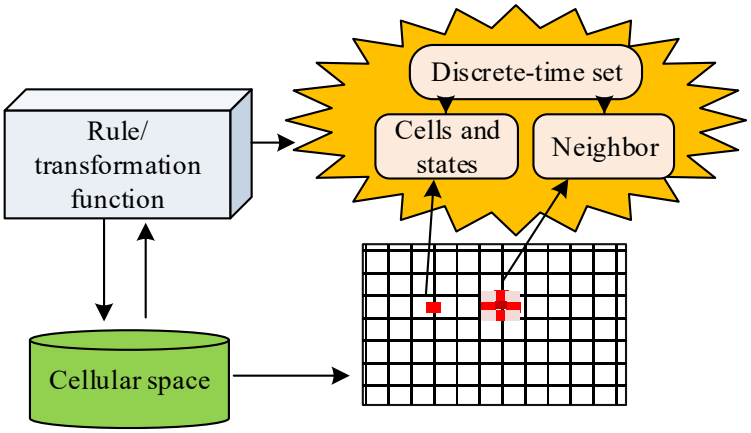

Figure 3. The composition of meta-cellular automata

In Figure 3, the meta-cellular automata model consists of four parts: grid cells, state sets, neighborhood definitions, and transition rules. Each cell updates its state based on the neighborhood state and rules, and the design of the transition rules is the core of the model. Based on the spatio-temporal characteristics of changes in the EEQ of the study area, combined with Markov chain theory, a state transition probability matrix (STPM) is constructed. Figure 4 depicts the Markov model's structure [25].

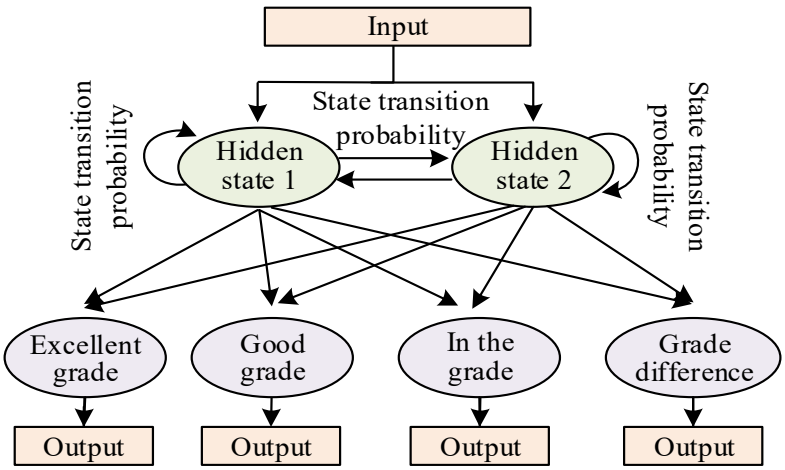

Figure 4. Markov model structure

In Figure 4, the Markov model consists of three parts: the state space, the STPM, and the initial state distribution. The state space defines the discrete state set of EEQ. The study categorizes quality levels into four classes: excellent, good, moderate, and poor. The state boundaries are determined based on time series analysis of historical RSD. The STPM is the core of the model, quantifying the probability of transitioning from the current state to the next state. The prediction process is shown in Equation 6.

$$S_{t+1} = S_t \cdot P \tag{6}$$

In Equation 6, S_{t+1} represents the state of the event during the $t+1$ period. S_t denotes the current state. P is the transition probability matrix. The study calculates the transition frequencies between states from 2021 to 2024 and constructs the probability matrix using the maximum likelihood estimation method. The initial state distribution is set based on the latest year's EEQ data. When integrating the meta-cellular automata model, the study uses the four grades of EEQ as the state set of the meta-cellular automata, and the neighborhood type adopts the common Moore neighborhood. The transition rules of the meta-cellular automata are shown in Equation 7.

$$S_{ij}^{\,t+1} = f\left(S_{ij}^{\,t}\right),\ P_{tran}, N_{ij}^{\,t} \tag{7}$$

In Equation 7, $S_{ij}^{\,t}$ is the EEQ grade status of location (i, j) at time t. $S_{ij}^{\,t+1}$ is the predicted status of location (i, j) at time $t+1$. P_{tran} is the STPM calculated by the Markov chain. $N_{ij}^{\,t}$ represents the neighborhood cell status set of location (i, j) at time t. f is the conversion function. The study introduces spatial distribution data of key influencing factors identified by GRA into the conversion function as constraint conditions. This can more accurately reflect the differences in driving forces behind changes in EEQ in different regions [26, 27]. The study will combine meta-cellular automata and Markov models as methods for prediction and evaluation. The study introduces a GWR model. This model uses spatial distribution data of key influencing factors to correct the STPM of the Markov chain locally. This correction more accurately reflects the non-stationary effects of driving factors on the state transition of EEQ at different spatial locations. The study combines the grey correlation method to identify the spatial distribution data of key influencing factors and uses them as constraints. Subsequently, the study uses a GWR model to establish a spatial coefficient relationship model between each driving factor and the probability of EEQ status transition. This model is shown in Equation 8.

$$P_{ij}(u,v) = b + \sum_{k=1}^{n} B_k(u,v) \cdot X_k(u,v) + \frac{E(u,v)}{H} \tag{8}$$

In Equation 8, $P_{ij}(u,v)$ represents the probability of transitioning from state i to state j at location (u,v). b is the intercept term. B is the regression coefficient of the kth driving factor X at location (u,v). E is the random error term. H is the corrected state transition probability. The study substitutes the corrected transition probability matrix into the cellular automaton transition rules, replacing the original global transition probability matrix. The specific process of the proposed tourism EEQ assessment method is shown in Figure 5 [28].

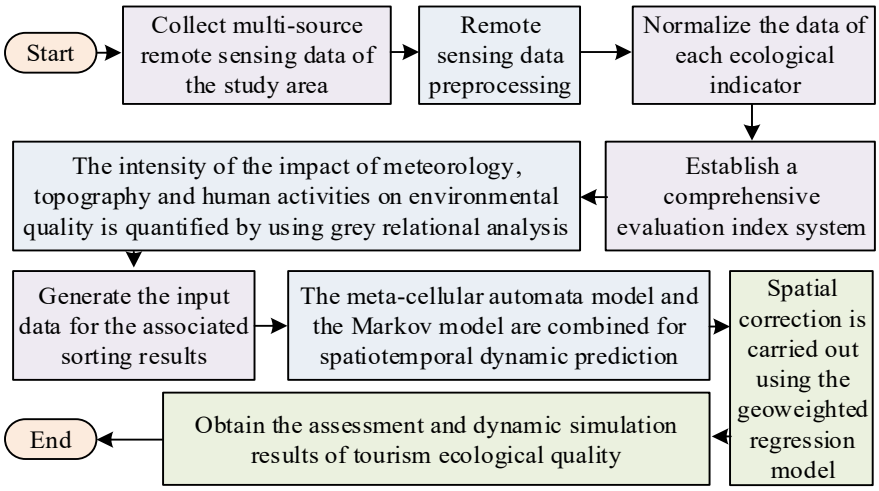

Figure 5. The specific process of the tourism EEQ assessment method proposed by the research

In Figure 5, the study first collects multi-source RS image data from the study area, including Landsat series and Sentinel data. The study then performs preprocessing steps, such as RC, AC, and GC, to eliminate noise and distortion. Key ecological indicators are then extracted using PCA. The study then normalizes vegetation indices, surface temperature, and humidity indices to construct a comprehensive EEQ assessment index system. On this basis, the GRA method is applied to quantify the impact intensity of meteorological, terrain, and human activities on EEQ, and the correlation ranking results are generated as input data. Subsequently, the study integrates the meta-cellular automata model and the Markov model for spatio-temporal dynamic prediction. The meta-cellular automata defines the state set as four quality levels: excellent, good, moderate, and poor, and adopts a Moore neighborhood structure. The Markov model provides a STPM, and the initial transition probabilities are calculated using maximum likelihood estimation based on historical data. To improve the accuracy of predictions and assessments, this study introduces a GWR model that corrects for spatial biases in Markov transition probabilities. The model establishes variable coefficient relationships using spatial distribution data of highly correlated factors and adjusts state transition rules to reflect regional differences. GWR is a local regression method that assigns different weights to different locations using a spatial weight matrix, effectively capturing spatial heterogeneity and enhancing model adaptability. The study uses the geographic weighted regression model to refine the transition probabilities for each grid cell, ensuring that the predicted results are more closely aligned with reality. A spatiotemporal distribution map of ecological and environmental quality is then produced when multi-temporal RSD is integrated to test the model's predicted accuracy and stability. Planning for tourism and regional ecological conservation have a scientific foundation thanks to this map.

In summary, this study constructs a dynamic assessment and prediction model for tourism ecological quality through multi-model fusion. The study first establishes an evaluation index system and index weight values based on grey correlation and PCA. The index weight values are then combined with RSD to simulate Eco-E changes through cellular automata, and a Markov model is used to predict future states. Finally, geographic weighted regression is used for spatial refinement adjustments to form comprehensive assessment results.

3. Results

To test the performance of the EEQ assessment method proposed in this study, a series of experiments are designed to analyze its performance. The advantages and disadvantages of the proposed method are discussed to provide an analytical basis for subsequent work.

3.1. Effectiveness Analysis of Improved Prediction Models

To improve the accuracy of the prediction model, the study introduces meta-cellular automata models and GWR models to optimize the Markov model. The study performs performance comparison studies between the classic Markov model, the meta-cellular automata-Markov model, and the improved model suggested in the study in an attempt to confirm the efficacy of the improved approach suggested in the study. The Kappa coefficient and spatial superposition accuracy rate of the three models are compared during the training process. In Figure 6(a), the Kappa coefficient of the improved model rises rapidly in the early stages of iteration and stabilizes after the 21st iteration, significantly higher than the other two models. Figure 6(b) displays that the spatial superposition accuracy rate of the improved model stabilizes after 23 iterations. The final convergence value is 92.34%, which is an improvement of 5.12% and 3.47% compared to the other two models. This indicates that the improved model is more predictive and stable in spatiotemporal dynamic simulations. This demonstrates the effectiveness of multi-model fusion and spatial heterogeneity correction.

Furthermore, the model's introduction of GWR demonstrates its excellent adaptability to different regions, effectively reflecting the characteristics of spatial non-stationarity.

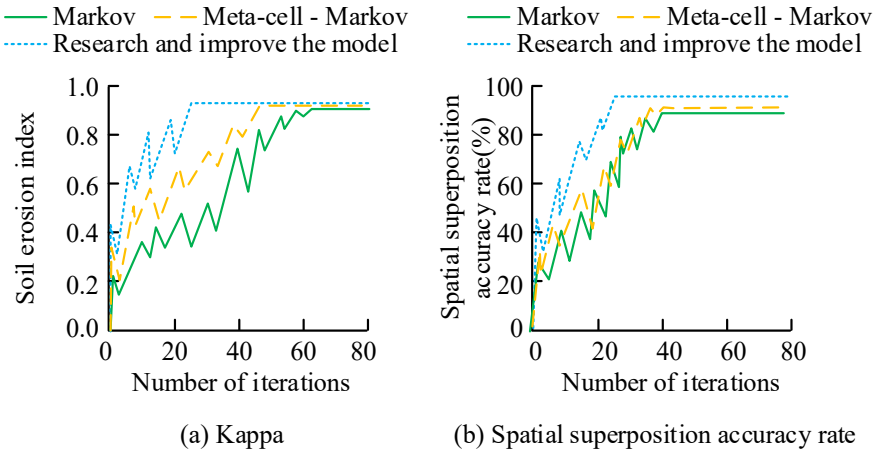

(a) Kappa (b) Spatial superposition accuracy rate

Figure 6. Comparison of the training results of the improved prediction model

To further validate the performance of the proposed improved method, the study conducts multiple independent experiments on different regions using random sampling. The selected regions include urban centers, suburbs, industrial zones, and ecological conservation areas. The evaluation indicators include root mean square error (RMSE), mean absolute percentage error (MAPE), Kappa coefficient, and spatial superposition accuracy rate. Table 4 displays the comparing results. The research design model performs optimally across all metrics, demonstrating high predictive accuracy and stability across different regions. Its average RMSE and MAPE values are 0.07 and 0.05, respectively, which are significantly lower than those of the other two models. Its average Kappa coefficient and spatial superposition accuracy rate are 0.93 and 93.34%, respectively, significantly higher than those of other models. The method proposed in the research introduces a GWR model to optimize spatial data processing, enhance the model's ability to capture local features, and improve prediction accuracy and consistency. Meanwhile, the introduction of metacellular automata enables the model to better simulate the nonlinear evolution process of complex land use changes and demonstrates stronger adaptability in spatial pattern reconstruction.

Table 4. Comparison of the generalization abilities of the three methods

Method		RMSE	MAPE	Kappa	Spatial superposition accuracy rate (%)
Urban central area	Markov model	0.32	0.18	0.78	79.34
	Meta-cell-Markov model	0.15	0.14	0.86	85.22
	Research design model	0.07	0.05	0.92	93.16
Suburb	Markov model	0.28	0.20	0.79	80.00
	Meta-cell-Markov model	0.20	0.15	0.86	84.57
	Research design model	0.06	0.06	0.93	93.64
Industrial zone	Markov model	0.30	0.19	0.77	79.54
	Meta-cell-Markov model	0.21	0.16	0.86	83.16
	Research design model	0.07	0.05	0.93	92.97
Ecological reserve	Markov model	0.27	0.20	0.80	80.11
	Meta-cell-Markov model	0.18	0.14	0.89	86.23
	Research design model	0.06	0.05	0.94	93.96

3.2. Assessment Results of EEQ in Tourist Areas

The changes in the EEQ assessment results in the study area from 2021 to 2024 are shown in Figure 7. Figure 7 (a) shows that in 2021, the proportion of areas (POAs) with poor quality is 25.3%, while the proportions of areas with moderate, good, and excellent quality are 32.1%, 28.6%, and 14.0%, respectively. In Figure 7(b), the POA classified as poor decreases to 20.7% in 2022, while the proportion classified as fair increases slightly to 33.5%. The proportions classified as good and excellent increase to 29.8% and 16.0%, respectively. In By 2023, Figure 7(c) shows that the

proportion of poor-quality areas decreases further to 16.5%. The proportion of average-quality areas remains stable at 33.8%. The proportions of good-quality and excellent-quality areas continue to increase, reaching 31.2% and 18.5%, respectively. As shown in Figure 7(d), by 2024, the POA classified as poor has declined to 12.4%, while the proportions of areas classified as moderate, good, and excellent are 32.9%, 32.7%, and 22.0%, respectively. The overall trend indicates continuous improvement in the EEQ in the study area from 2021 to 2024. A notable decrease in the region categorized as poor and a consistent rise in the area labeled as exceptional are characteristics of this progress. This is a changing trend closely related to the continuous advancement of ecological protection measures within the region, especially the implementation of ecological restoration projects, the effective control of pollution sources, and the continuous improvement of the green space system. The experimental results show that the average annual improvement rate of the EEQ index in the study area is 2.3%. The improvement rate accelerated by 1.2 percentage points from 2023 to 2024 compared to the previous period. This reflects the effectiveness of the governance measures. Spatial analysis reveals that areas with superior grades primarily expand along the greenway network, whereas areas with poor grades transition from isolated pockets to edge retreat.

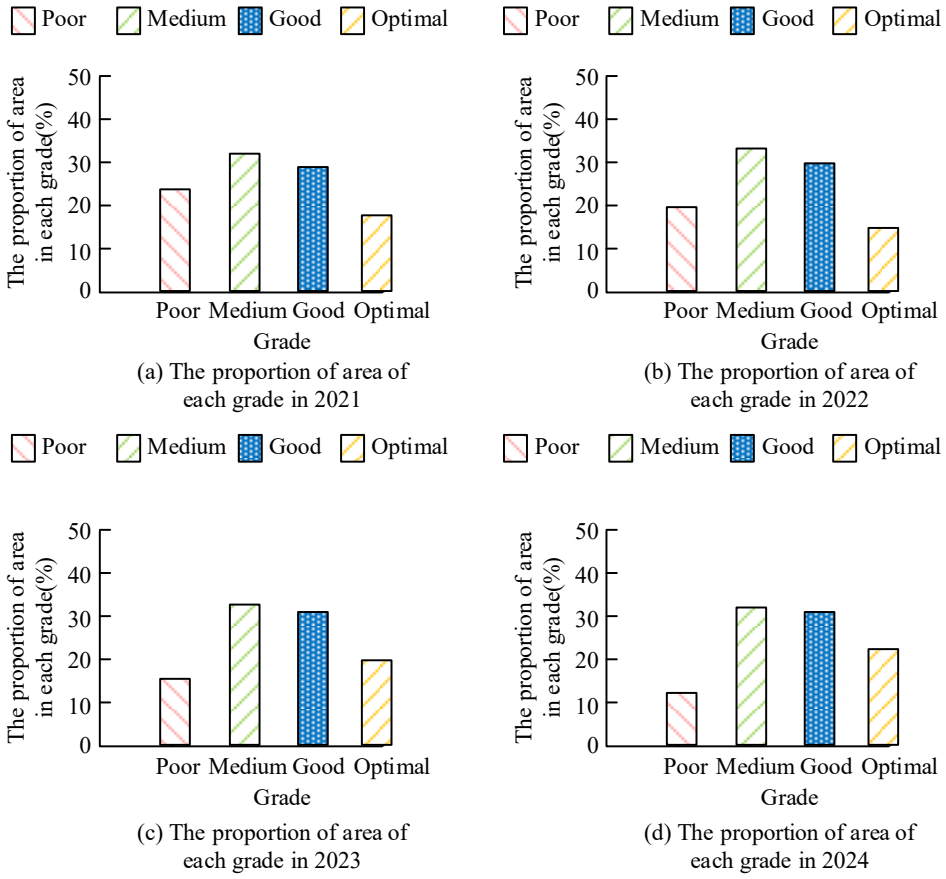

Figure 7. The changes in the EEQ assessment results of the study area from 2021 to 2024

The initial state of the model is set as the spatial distribution map of the EEQ grade of the study area in 2024. The study sets the simulation step length to one year and simulates and predicts the spatio-temporal changes in the EEQ of the study area from 2025 to 2030. The study forecasts the region's EEQ in 2022 using historical data from the previous 12 months in 2021 to confirm the model's prediction accuracy. It then compares this with the actual assessment results. The study compares the proposed prediction evaluation method (Method 1) with the evaluation methods in Li et al. [29] (Method 2), Moilanen et al. [30] (Method 3), Wu & Wang [31] (Method 4), and Song et al. [32] (Method 5). In Figure 8(a), the overall EEQ of the study area will continue to improve between 2025 and 2030, but the rate of improvement will slow down. The POA with poor EEQ is expected to steadily decline from 10.3% in 2025 to 7.2% in 2030. The POA with moderate EEQ will remain relatively stable, fluctuating between 32.5% and 33.1%. The POA classified as “good” will increase slightly, from 33.5% in 2025 to 34.8% in 2030. The most significant growth will be observed in areas classified as “excellent,” with their proportion expected to rise from 23.7% in 2025 to 27.0% in 2030. The model’s predictions are broadly consistent with historical trends observed between 2021 and 2024. In Figure 8(b), the goodness of fit for Method 1 reaches 0.95, while the fit degree for Methods 2, 3, 4, and 5 are 0.83, 0.86, 0.80, and 0.78, respectively, which are significantly lower than the performance of Method 1. This indicates that the cellular automator-Markov model with integrated geographic weighted regression correction proposed in the research is superior to the existing methods in terms of prediction accuracy. This is attributed to the model's effective characterization of spatial heterogeneity and precise capture of local driving factor effects. This verifies the model's reliability and superiority in dynamically predicting EEQ.

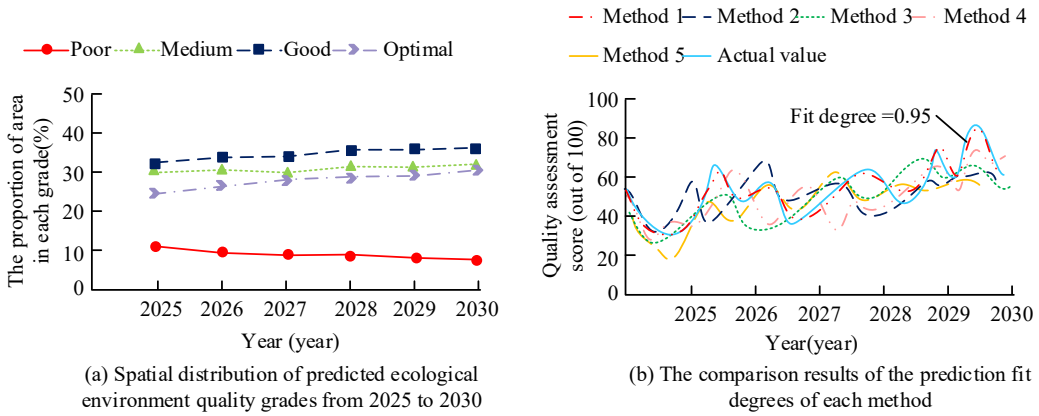

(a) Spatial distribution of predicted ecological environment quality grades from 2025 to 2030

(b) The comparison results of the prediction fit degrees of each method

Figure 8. The spatio-temporal variation pattern of the EEQ in the study area and the fitting of the prediction results

To further evaluate the performance of the proposed method, Kappa coefficients, overall accuracy (OA), RMSE, and R^2 are compared among the different methods. The changes in performance metrics of each method are also examined as the amount of data increases. In Figure 9(a), as the amount of data increases, the Kappa coefficients of each method gradually decrease, with Method 1 showing the smallest decrease. Its average Kappa coefficient value is 0.85. In Figure 9(b), the prediction results of the methods are basically consistent with the actual results, with an overall OA value of 91.35%, meeting the accuracy requirements. Compared with other methods, Method 1 has a higher OA value. In Figure 9(c), the RMSE value of Method 1 is only 0.08, and its error curve remains below the error curves of other methods throughout. In Figure 9(d), Method 1 has an R^2 value of 0.94, outperforming all other methods. This indicates that Method 1 demonstrates significant advantages in multi-dimensional performance evaluation, validating its efficiency and reliability in EEQ prediction. As the amount of data increases, Method 1 maintains high stability, further highlighting its superiority. This performance is attributed to its adaptive adjustment mechanism for spatial non-stationarity and its capability to fuse multi-source data. Its generalization performance in complex environments significantly outperforms traditional models. It can maintain the robustness and consistency of the prediction results even under conditions of data redundancy or uneven distribution, demonstrating its strong practical applicability and promotion potential.

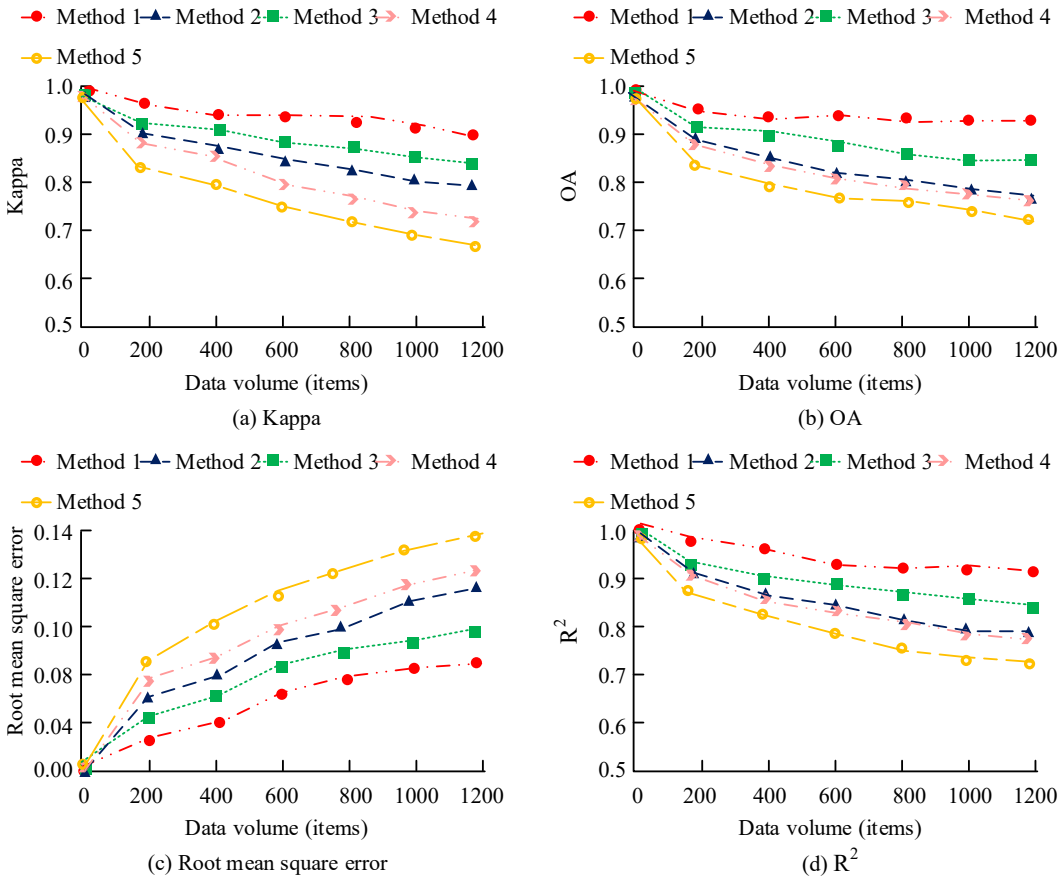

(a) Kappa

(b) OA

(c) Root mean square error

(d) R^2

Figure 9. The comparison results of Kappa coefficients and OA of each method

3.3. Application effectiveness of tourism EEQ assessment methods

To further test the effectiveness of the proposed tourism EEQ assessment method, the study applies it to actual EEQ assessment scenarios. The study selects A typical tourist area in Location A as the experimental object and applied five methods to the real-time assessment of EEQ. The experimental period is one year, with a comprehensive assessment conducted every three months. The dataset used for the experiment spans from January to December of 2024 and includes 12 assessment periods. This dataset contains environmental data from various seasons and peak tourist periods. There are 16,743 pieces of data, including indicators such as temperature, humidity, PM2.5 concentration, noise value, vegetation coverage and tourist density. The study introduces benchmarking as a reference, with the benchmark method being the traditional expert scoring method. The study selects five experts with rich experience in the field of ecology and the environment to conduct independent scoring, and compares the results with those of each method. During the experiment, the fit between the evaluation results of each method and the expert scores, as well as the response delay time of each method, are shown in Figure 10. In Figure 10(a), the evaluation results of Method 1 have the highest fit with the expert scores, with an average fit of 0.89. Furthermore, as the experiment progresses, the fit fluctuates the least, demonstrating significant stability. With an average of just 2.5 s, Method 1 has the smallest reaction delay time in Figure 10(b), which is far less than the average delay periods of the other techniques. This indicates that Method 1 performs exceptionally well in terms of real-time capability and stability, effectively addressing complex and dynamic changes in Eco-Es, and providing precise and efficient assessment support for tourist areas.

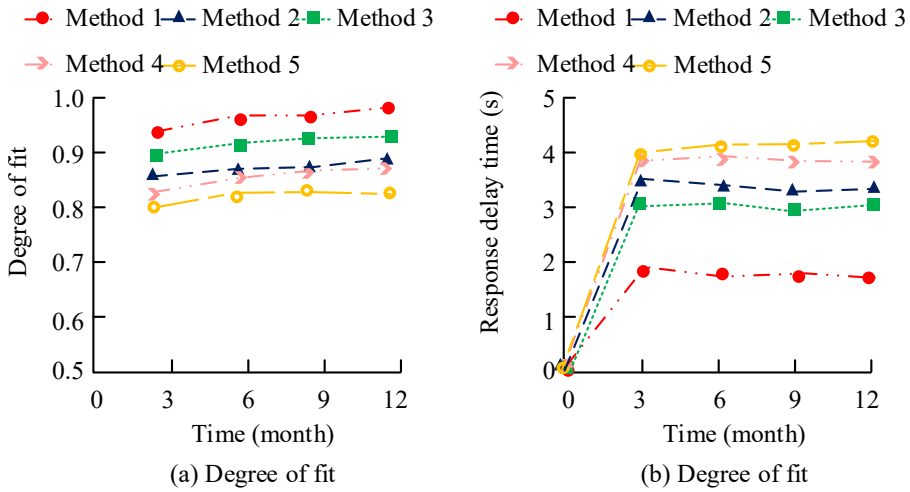

Figure 10. Comparison of the practical application effects of each method

To test the robustness of the proposed methods, the study selects Region B in the northeast, Region C in the northwest, and Region D in the southeast for cross-regional validation. The fit and response time of the evaluation results of each method in the four regions are compared. Table 5 displays the comparing results. Method 1 demonstrates the best fit and shortest response time in all regions, verifying its universality and efficiency. Its average fit value is 0.90, and its average response time is 2.53 s, significantly better than other methods. In contrast, other methods show significant fluctuations in different regions, further highlighting the superiority of Method 1 in complex environments. This indicates that Method 1 not only demonstrates outstanding performance in specific regions but also shows high adaptability and stability under diverse geographical and ecological conditions. Its core algorithm has strong generalization ability for different environmental characteristics. This feature effectively overcomes assessment interference caused by regional differences. It ensures consistent and reliable results and provides solid technical support for dynamic monitoring and scientific decision-making regarding cross-regional tourism Eco-Es.

Table 5. Comparison of cross-regional evaluation results of each method

Project	A		B		C		D	
	Degree of fit	Response time (s)	Degree of fit	Response time (s)	Degree of fit	Response time (s)	Degree of fit	Response time (s)
Method 1	0.90	2.54	0.89	2.56	0.89	2.49	0.91	2.55
Method 2	0.81	3.27	0.82	3.30	0.81	3.45	0.80	3.50
Method 3	0.86	2.98	0.84	3.00	0.81	3.15	0.85	3.00
Method 4	0.75	3.77	0.74	3.80	0.73	3.75	0.72	3.68
Method 5	0.71	4.00	0.71	4.12	0.70	4.20	0.72	4.33

To further validate the practical performance of the proposed method, the study compares the evaluation results of different methods in different seasons. The comparison indicators include the Kappa coefficient, OA value, RMSE, R^2 value, MAPE, and evaluation accuracy. Table 6 displays the findings. Under different seasonal conditions, Method 1 outperforms other methods in all metrics, with particularly notable performance in winter and summer. The average values for its Kappa, OA, RMSE, R^2, MAPE, and evaluation accuracy metrics are 0.93, 0.93, 0.07, 0.91, 0.08, and 93.88%, respectively. The data in Table 6 show that Method 1 maintains high Kappa and OA values and low error rates in all seasons (spring, autumn, winter, and summer), with an accuracy rate consistently above 93%, significantly outperforming other methods. The study suggests that the method can effectively address the challenges posed by environmental changes, ensuring the accuracy and consistency of data processing.

Table 6. Comparison of the practical application effects of various methods in different seasons

Project		Kappa	OA	RMSE	R^2	MAPE	Evaluation accuracy (%)
Spring and Autumn	Method 1	0.93	0.94	0.08	0.90	0.07	94.20
	Method 2	0.87	0.88	0.19	0.82	0.15	88.47
	Method 3	0.89	0.90	0.13	0.85	0.12	90.03
	Method 4	0.85	0.85	0.23	0.80	0.20	85.72
	Method 5	0.80	0.81	0.25	0.76	0.20	83.41
Winter and summer	Method 1	0.93	0.93	0.07	0.91	0.08	93.88
	Method 2	0.86	0.85	0.19	0.82	0.18	88.43
	Method 3	0.89	0.88	0.14	0.86	0.15	90.00
	Method 4	0.84	0.81	0.23	0.77	0.23	83.12
	Method 5	0.81	0.80	0.27	0.73	0.26	80.84

To further verify the performance of the proposed method in the research, the experiment introduces more comprehensive evaluation indicators and comparison methods. The methods from Shu et al. [15] and Zhou et al. [17] are introduced and set as Method 6 and Method 7 respectively for comparative analysis. Moreover, the performance of each method is tested and compared in more complex scenarios. The introduced indicators in the study include R^2, RMSE, MAPE, and Kappa coefficient. In addition, there are assessment accuracy and overall consistency. The comparison scenarios include high-density urban building areas, urban-rural fringe areas, and complex terrain regions. The results show that compared with Methods 2 to 7, Method 1 is more stable and adaptable in various scenarios. Its R^2 value remains above 0.91, RMSE is below 0.09, MAPE does not exceed 8%, Kappa coefficient is stable above 0.85, and the evaluation accuracy exceeds 93% in all cases. Especially in the high-density building areas of cities, the overall consistency of Method 1 is approximately 4.2 % higher than that of the suboptimal method. In the urban-rural fringe area, Method 1's R^2 reached 0.92, which is 0.06 higher than Method 6's. The MAPE decreases to 7.3%, making Method 1 significantly superior to the others. In the complex terrain area, its Kappa coefficient is 0.87, and the assessment accuracy remains above 94.1%. The specific results are shown in Table 7.

Table 7. Performance Comparison results of each method in different scenarios

Method		R^2	RMSE	MAPE (%)	Kappa	Evaluation accuracy (%)	Overall consistency
High-density building areas in cities	Method 1	0.93	0.07	7.1	0.88	94.2	0.89
	Method 6	0.87	0.13	9.8	0.79	89.5	0.84
	Method 7	0.85	0.15	10.2	0.77	87.3	0.81
Urban-rural fringe	Method 1	0.92	0.08	7.3	0.86	93.8	0.87
	Method 6	0.86	0.14	9.9	0.78	88.4	0.82
	Method 7	0.84	0.16	10.5	0.75	86.7	0.80
Complex terrain area	Method 1	0.91	0.09	7.8	0.87	94.1	0.88
	Method 6	0.83	0.17	11.1	0.74	85.9	0.81
	Method 7	0.81	0.19	12.3	0.72	84.2	0.79

The spatial and temporal resolutions of remote sensing data refer to the minimum distance a sensor can distinguish between two adjacent ground objects and the time interval for repeatedly observing the same area, respectively. Higher spatial resolution provides clearer details of ground objects and improves identification accuracy in areas with dense buildings. Higher temporal resolution means a faster data update frequency, which facilitates the dynamic monitoring of land use changes in urban-rural fringe areas. The synergy of the two can effectively reduce the misjudgment rate in complex terrains and enhance the stability of the model.

To detect the sensitivity of the proposed research methods to changes in index weights or parameter values (such as Markov transition probabilities, etc.), multiple sets of comparative experiments are designed. The fluctuation of the model's output results is observed by adjusting the weight coefficients of each influencing factor. Experiments show that within a parameter variation range of ±30%, the Kappa coefficient of Method 1 always remains above 0.85, verifying its good robustness and adaptability.

4. Discussion

To achieve accurate and efficient assessment of tourism ecological quality, this study proposed a method based on PCA and RSD. This method combined the results of PCA and the grey-scale correlation method to construct a comprehensive assessment model. Based on this, dynamic simulation and prediction were achieved by combining the meta-cellular automata model and the Markov model. Current research centered on natural and humanistic aspects explores key factors affecting EEQ. Analysis results indicated that the Kappa coefficient of the improved model tended to stabilize after the 21st iteration, reaching a value of 0.92. The spatial superposition accuracy rate of the improved model tended to stabilize after 23 iterations, with a final convergence value of 92.34%. The stability and precision of the enhanced model were noticeably better than those of the conventional model.

When evaluating historical data, Method 1 achieved a goodness-of-fit of 0.95. In contrast, Methods 2, 3, 4, and 5 had fit degrees of 0.83, 0.86, 0.80, and 0.78, respectively, which were significantly lower than Method 1's performance. In the analysis results across different data scales, as the data volume increased, Method 1's average Kappa coefficient value was 0.85. Its overall OA value was 91.35%, meeting the accuracy requirements. The RMSE value of Method 1 is only 0.08, and the R^2 of Method 1 was 0.94, both of which outperformed other methods. In practical applications, the average values of the Kappa, OA, RMSE, R^2, MAPE, and evaluation accuracy metrics for Method 1 were 0.93, 0.93, 0.07, 0.91, 0.08, and 93.88%, respectively. Compared to other methods, Method 1 demonstrated higher stability and reliability across all metrics.

The research results showed that improving the green value directly reflected an increase in vegetation coverage and an improvement in the quality of the Eco-E. During the construction of urban green spaces and ecological restoration projects, remote sensing monitoring showed that the vegetation index had continuously risen, indicating that the ecosystem was gradually returning to stability. Through time series analysis, it was found that the correlation between changes in green values and climate factors, such as temperature and precipitation, was significant. This revealed the mechanism by which the synergistic effects of natural conditions and human activities influenced the Eco-E. In addition, there were differentiated characteristics of the evolution of EEQ in different spatial regions. Therefore, when formulating ecological protection policies, it was necessary to implement differentiated management strategies that took into account the region's actual conditions, including the spatio-temporal heterogeneity of the climate, land use patterns, and the intensity of human activities. Current research has only considered the impact of natural and human factors on the Eco-E. In future research, factors such as policy and economic development could be further incorporated to enhance the accuracy of assessment results. Additionally, machine learning and big data technologies could be used to continuously optimize the model and enhance its adaptive capabilities.

5. Conclusion

The tourism EEQ assessment method based on principal component analysis proposed by the research was significantly superior to the traditional model in terms of stability and accuracy, and had high practical value. Compared to other methods, the research design method performed better and was more stable in different seasons. The average values of its Kappa, OA, RMSE, R^2, MAPE and evaluation accuracy rate indicators were 0.93, 0.93, 0.07, 0.91, 0.08, and 93.88%, respectively. When evaluating historical data, its fitting degree reached 0.95. During the training process, the Kppa coefficient of the improved model tended to stabilize after the 21st iteration, reaching a value of 0.92. The spatial overlay accuracy rate of the improved model tended to stabilize after 23 iterations, and the final convergence value was 92.34%. Moreover, in experiments conducted in urban high-density areas, urban fringe areas, and complex terrain regions, Method 1 demonstrated an overall consistency that was approximately 4.2 % higher than the suboptimal method. In the urban-rural fringe area, the R^2 of Method 1 reached 0.92, which was 0.06 higher than that of method 6, and the MAPE decreased to 7.3%, significantly superior to other methods. In the complex terrain area, its Kappa coefficient was 0.87, and the assessment accuracy remained above 94.1%.

Based on the experimental results above, it is evident that the proposed method can provide a scientific basis for planning and managing ecotourism areas, helping to achieve SD goals. By integrating this model into the geographic information system platform, decision-makers can achieve dynamic monitoring and visual management of the quality of the regional Eco-E. By integrating multi-temporal data input, the model can generate quarterly or annual assessment reports to assist in formulating ecological protection priorities and tourism development strategies. Meanwhile, by setting a threshold early warning mechanism, an alarm is automatically triggered when key indicators deviate from the normal range, thereby enhancing response efficiency. In addition, the output results of the model can directly support policy evaluation and cross-departmental collaborative decision-making, promoting the formation of a scientific and refined ecological governance system. For example, when developing tourism projects in ecologically sensitive areas, decision-makers can use the model's spatio-temporal heat map output to identify potential risk areas and optimize project site selection and tourist carrying capacity.

6. Declarations

6.1. Author Contributions

Conceptualization, R.C. and X.W.; methodology, R.C.; validation, R.C., X.W., and W.W.; data curation, R.C.; writing—original draft preparation, R.C.; writing—review and editing, R.C.; funding acquisition, X.W. All authors have read and agreed to the published version of the manuscript.

6.2. Data Availability Statement

The data presented in this study are available in the article.

6.3. Funding

The research is supported by Guangdong Province Higher Education Institutions Key Research Platforms and Projects - Key Areas Specialized Projects (Science and Technology Serving Rural Revitalization): Research on Ecological Erosion and Cultural Ecology Conservation in Traditional Waterfront Villages of Guangdon (2021ZDZX4069); Ministry of Education, Department of Student Affairs Supply-Demand Matching Employment and Education Project: Research on Talent Cultivation Models for Industry-Education Integration in Hospitality and Tourism at Higher Vocational Colleges Under the Digital Economy (20230110164).

6.4. Institutional Review Board Statement

Not applicable.

6.5. Informed Consent Statement

Not applicable.

6.6. Declaration of Competing Interest

The authors declare that they have no known competing financial interests or personal relationships that could have appeared to influence the work reported in this paper.

7. References

[1] Xue, B., Han, B., Li, H., Gou, X., Yang, H., Thomas, H., & Stückrad, S. (2023). Understanding ecological civilization in China: From political context to science. Ambio, 52(12), 1895–1909. doi:10.1007/s13280-023-01897-2.

[2] Ge, X., Ding, J., Teng, D., Wang, J., Huo, T., Jin, X., Wang, J., He, B., & Han, L. (2022). Updated soil salinity with fine spatial resolution and high accuracy: The synergy of Sentinel-2 MSI, environmental covariates and hybrid machine learning approaches. Catena, 212(3), 106054–106068. doi:10.1016/j.catena.2022.106054.

[3] Cai, Z., Zhang, Z., Zhao, F., Guo, X., Zhao, J., Xu, Y., & Liu, X. (2023). Assessment of eco-environmental quality changes and spatial heterogeneity in the Yellow River Delta based on the remote sensing ecological index and geo-detector model. Ecological Informatics, 77(3), 102203–102215. doi:10.1016/j.ecoinf.2023.102203.

[4] Yoshe, A. K. (2023). Groundwater Potential Zone Identification Using Remote-Sensing based/GIS Based Machine and Analytical Hierarchy Process (AHP) for Abbay Watershed, East Africa. Engineering Heritage Journal, 7(1), 10–25. doi:10.26480/gwk.01.2023.10.25.

[5] Ogbeibu, S., Emelifeonwu, J., Pereira, V., Oseghale, R., Gaskin, J., Sivarajah, U., & Gunasekaran, A. (2024). Demystifying the roles of organisational smart technology, artificial intelligence, robotics and algorithms capability: A strategy for green human resource management and environmental sustainability. Business Strategy and the Environment, 33(2), 369–388. doi:10.1002/bse.3495.

[6] Wu, H., Chen, C., Liao, L., Hou, J., Sun, W., Yan, Q., Gu, J., & Lin, W. (2023). Neighbourhood Representative Sampling for Efficient End-to-End Video Quality Assessment. IEEE Transactions on Pattern Analysis and Machine Intelligence, 45(12), 15185–15202. doi:10.1109/TPAMI.2023.3319332.

[7] Sun, C., Li, J., Liu, Y., Cao, L., Zheng, J., Yang, Z., Ye, J., & Li, Y. (2022). Ecological quality assessment and monitoring using a time-series remote sensing-based ecological index (TS-RSEI). GIScience and Remote Sensing, 59(1), 1793–1816. doi:10.1080/15481603.2022.2138010.

[8] Li, S., & Fan, Z. (2022). Evaluation of urban green space landscape planning scheme based on PSO-BP neural network model. Alexandria Engineering Journal, 61(9), 7141–7153. doi:10.1016/j.aej.2021.12.057.

[9] Zhang, C., & Eskandarian, A. (2023). A Quality Index Metric and Method for Online Self-Assessment of Autonomous Vehicles Sensory Perception. IEEE Transactions on Intelligent Transportation Systems, 24(12), 13801–13812. doi:10.1109/TITS.2023.3303320.

[10] Lines, E. R., Fischer, F. J., Owen, H. J. F., & Jucker, T. (2022). The shape of trees: Reimagining forest ecology in three dimensions with remote sensing. Journal of Ecology, 110(8), 1730–1745. doi:10.1111/1365-2745.13944.

[11] Pan, X., Cao, M., Zheng, L., Xiao, Y., Qi, L., Xing, Q., Kim, K., Sun, D., Wang, N., Guo, M., Wu, M., Li, X., Yuan, C., Qing, S., Qiu, Z., Lu, Y., Wang, C., Ren, P., Cai, X., … Cui, T. (2024). Remote Sensing of Ulva Prolifera Green Tide in the Yellow Sea Using Multisource Satellite Data: Progress and prospects. IEEE Geoscience and Remote Sensing Magazine, 12(4), 110–131. doi:10.1109/MGRS.2024.3364678.

[12] Lu, H., Lu, X., Jiao, L., & Zhang, Y. (2022). Evaluating urban agglomeration resilience to disaster in the Yangtze Delta city group in China. Sustainable Cities and Society, 76(2), 103464–103472. doi:10.1016/j.scs.2021.103464.

[13] Yu, Z., Wang, J., Chen, H., & Yamani Idna Idris, M. (2025). QRS-TRS: Style Transfer-Based Image-to-Image Translation for Carbon Stock Estimation in Quantitative Remote Sensing. IEEE Access, 13(1), 52726–52737. doi:10.1109/ACCESS.2025.3554045.

[14] Pan, J., Chen, T., Jia, K., & Plaza, A. (2025). Toward Sustainable Mining Landscapes: Evaluating Spatiotemporal Changes and Driving Mechanisms of Eco-Environmental Quality in Central China. IEEE Journal of Selected Topics in Applied Earth Observations and Remote Sensing, 18(2), 21144–21155. doi:10.1109/JSTARS.2025.3599164.

[15] Shu, P., Aslam, R. W., Naz, I., Ghaffar, B., Kucher, D. E., Quddoos, A., Raza, D., Abdullah-Al-Wadud, M., & Zulqarnain, R. M. (2025). Deep Learning-Based Super-Resolution of Remote Sensing Images for Enhanced Groundwater Quality Assessment and Environmental Monitoring in Urban Areas. IEEE Journal of Selected Topics in Applied Earth Observations and Remote Sensing, 18(1), 7933–7949. doi:10.1109/JSTARS.2025.3548010.

[16] Han, H., Liu, Z., Li, J., & Zeng, Z. (2024). Challenges in remote sensing based climate and crop monitoring: navigating the complexities using AI. Journal of Cloud Computing, 13(1), 1–14. doi:10.1186/s13677-023-00583-8.

[17] Zhou, D., Sheng, M., Bao, C., Hao, Q., Ji, S., & Li, J. (2024). 6G Non-Terrestrial Networks-Enhanced IoT Service Coverage: Injecting New Vitality into Ecological Surveillance. IEEE Network, 38(4), 63–71. doi:10.1109/MNET.2024.3382246.

[18] Anderle, M., Brambilla, M., Hilpold, A., Matabishi, J. G., Paniccia, C., Rocchini, D., Rossin, J., Tasser, E., Torresani, M., Tappeiner, U., & Seeber, J. (2023). Habitat heterogeneity promotes bird diversity in agricultural landscapes: Insights from remote sensing data. Basic and Applied Ecology, 70(2), 38–49. doi:10.1016/j.baae.2023.04.006.

[19] Yue, G., Cheng, D., Zhou, T., Hou, J., Liu, W., Xu, L., Wang, T., & Cheng, J. (2023). Perceptual Quality Assessment of Enhanced Colonoscopy Images: A Benchmark Dataset and an Objective Method. IEEE Transactions on Circuits and Systems for Video Technology, 33(10), 5549–5561. doi:10.1109/TCSVT.2023.3260212.

[20] Wang, J., Zhen, J., Hu, W., Chen, S., Lizaga, I., Zeraatpisheh, M., & Yang, X. (2023). Remote sensing of soil degradation: Progress and perspective. International Soil and Water Conservation Research, 11(3), 429–454. doi:10.1016/j.iswcr.2023.03.002.

[21] Li, Q., Yang, T., & Li, L. (2022). Evaluation of snow depth and snow cover represented by multiple datasets over the Tianshan Mountains: Remote sensing, reanalysis, and simulation. International Journal of Climatology, 42(8), 4223–4239. doi:10.1002/joc.7459.

[22] Wakjira, T. G., Kutty, A. A., & Alam, M. S. (2024). A novel framework for developing environmentally sustainable and cost-effective ultra-high-performance concrete (UHPC) using advanced machine learning and multi-objective optimization techniques. Construction and Building Materials, 416(2), 135114–135120. doi:10.1016/j.conbuildmat.2024.135114.

[23] Guo, H., Liang, D., Sun, Z., Chen, F., Wang, X., Li, J., Zhu, L., Bian, J., Wei, Y., Huang, L., Chen, Y., Peng, D., Li, X., Lu, S., Liu, J., & Shirazi, Z. (2022). Measuring and evaluating SDG indicators with Big Earth Data. Science Bulletin, 67(17), 1792–1801. doi:10.1016/j.scib.2022.07.015.

[24] Curnick, D. J., Davies, A. J., Duncan, C., Freeman, R., Jacoby, D. M. P., Shelley, H. T. E., Rossi, C., Wearn, O. R., Williamson, M. J., & Pettorelli, N. (2022). SmallSats: a new technological frontier in ecology and conservation? Remote Sensing in Ecology and Conservation, 8(2), 139–150. doi:10.1002/rse2.239.

[25] Guo, B., Lu, M., Fan, Y., Wu, H., Yang, Y., & Wang, C. (2023). A novel remote sensing monitoring index of salinization based on three-dimensional feature space model and its application in the Yellow River Delta of China. Geomatics, Natural Hazards and Risk, 14(1), 95–116. doi:10.1080/19475705.2022.2156820.

[26] Ke, L., Liu, D., Tan, Q., Wang, S., Wang, Q., & Yang, J. (2024). Spatial-Temporal Pattern of Land Use and SDG15 Assessment in the Bohai Rim Region Based on GEE and RF Algorithms. IEEE Journal of Selected Topics in Applied Earth Observations and Remote Sensing, 17(1), 7541–7553. doi:10.1109/JSTARS.2024.3380580.

[27] Usman, A. M., & Abdullah, M. K. (2023). An Assessment of Building Energy Consumption Characteristics Using Analytical Energy and Carbon Footprint Assessment Model. Green and Low-Carbon Economy, 1(1), 28–40. doi:10.47852/bonviewglce3202545.

[28] Yao, K., Halike, A., Chen, L., & Wei, Q. (2022). Spatiotemporal changes of eco-environmental quality based on remote sensing-based ecological index in the Hotan Oasis, Xinjiang. Journal of Arid Land, 14(3), 262–283. doi:10.1007/s40333-022-0011-2.

[29] Li, X., Yi, S., Cundy, A. B., & Chen, W. (2022). Sustainable decision-making for contaminated site risk management: A decision tree model using machine learning algorithms. Journal of Cleaner Production, 371(1), 133612–133625. doi:10.1016/j.jclepro.2022.133612.

[30] Moilanen, A., Lehtinen, P., Kohonen, I., Jalkanen, J., Virtanen, E. A., & Kujala, H. (2022). Novel methods for spatial prioritization with applications in conservation, land use planning and ecological impact avoidance. Methods in Ecology and Evolution, 13(5), 1062–1072. doi:10.1111/2041-210X.13819.

[31] Wu, X., & Wang, Z. (2022). Multi-objective optimal allocation of regional water resources based on slime mould algorithm. Journal of Supercomputing, 78(16), 18288–18317. doi:10.1007/s11227-022-04599-w.

[32] Song, Y., Gao, Y., Zhang, S., Dong, H., & Liu, X. (2024). Research on the Coupling Coordination and Driving Mechanisms of New-Type Urbanization and the Ecological Environment in China's Yangtze River Delta. Sustainability (Switzerland), 16(13), 5308–5320. doi:10.3390/su16135308.